Protective Effects of a Quercetin-Rich Fluorocarbon-Modified Chitosan Eyedrop from Radish (*Raphanus sativus* L.) Leaves Against Streptozotocin-induced Diabetic Retinopathy in Rats: An In Silico and In Vivo Study

Zahra Ramadhani[1], Setia Nurhidayah[1], Husnul Fikri[1], Dzaki Ahmad Lubis[1], Kaysha Natania Nurdin Putri[1], Humairah Medina Liza Lubis[1*]

[1] Department of Anatomical Pathology, Faculty of Medicine and Health Sciences, Universitas Muhammadiyah Sumatera Utara, Medan, Indonesia
humairamedina@umsu.ac.id

Abstract. Diabetic retinopathy (DR) is a major microvascular complication of diabetes, in which chronic hyperglycaemia, oxidative stress, and vascular endothelial growth factor A (VEGF-A) overexpression drive pathological retinal angiogenesis. Current anti-VEGF therapy requires repeated intravitreal injections, motivating the search for noninvasive alternatives. This study developed and evaluated a topical quercetin eye drop derived from radish (Raphanus sativus L.) leaves, encapsulated in fluorocarbon-modified chitosan (FCS), using in silico, physicochemical, and in vivo assessments. Molecular docking against VEGF-A (PDB 3QTK) showed that quercetin had the second most favourable binding energy (−8.21 kcal/mol; inhibition constant 9.089 μM) among the four candidate flavonols, after the anti-VEGF comparator faricimab (−8.93 kcal/mol), and shared several binding pocket residues with it. Leaves extracted by 70% ethanol maceration yielded 23.20% extract (moisture 7.85%) with positive flavonoid, alkaloid, saponin, tannin, triterpenoid, and phenolic reactions; HPLC confirmed quercetin at 125.430 ppm. The FTIR spectrum of the FCS carrier showed an FTIR spectrum 99.48% correlation with the chitosan standard. Three eye drop variants containing 100, 50, and 25 mg of extract (V1–V3) were clear, odourless, and sterile liquids at pH 7, with viscosities of 2.809, 2.505, and 2.214 cP; mean particle size was 24.67 nm, encapsulation efficiency ranged from 84.72–93.85%, and refractive indices fell within the accepted ocular range. In streptozotocin-induced diabetic rats, the highest-dose formulation (P1) produced the greatest fasting blood glucose reduction (62.47 ± 0.45%) and the lowest retinal histopathological damage score (4.00 ± 0.63) compared with the diabetic control (14.33 ± 1.21; Kruskal–Wallis test, $p < 0.05$). These findings provide preliminary, biologically plausible evidence that quercetin-FCS eye drops may protect against diabetic retinal injury, supported in silico by favourable VEGF-A binding affinity; however, direct in vivo VEGF quantification is still required before a VEGF-targeted mechanism can be confirmed.

© The Author(s) 2026
F. Maulina and S. Wahyuni (eds.), *Proceedings of the 3rd Malikussaleh International Conference on Health and Disaster Medicine (MICOHEDMED 2026)*, Advances in Health Sciences Research 97,
https://doi.org/10.2991/978-94-6239-836-8_10

Keywords: Quercetin, Raphanus sativus L., Fluorocarbon-Modified Chitosan, Molecular Docking, VEGF-A, Diabetic Retinopathy, Ocular Drug Delivery.

1 Introduction

Diabetic retinopathy (DR) is a chronic retinal complication of diabetes mellitus and a leading cause of visual impairment worldwide. The 11th edition of the International Diabetes Federation (IDF) Diabetes Atlas estimates that the global prevalence of diabetes will continue to rise sharply through 2050, with Indonesia among the countries contributing substantially to this burden [1]. Chronic hyperglycaemia induces oxidative stress, inflammatory signalling, endothelial dysfunction, capillary non-perfusion, pericyte loss, microaneurysm formation, and, in advanced disease, pathological retinal neovascularisation.

Vascular endothelial growth factor A (VEGF-A) is a key mediator of this process. Its expression is upregulated by chronic hyperglycaemia and hypoxia, which in turn promotes pathological neovascularisation and excessive vascular permeability through pathways such as PKC/ET/NF-κB/ICAM-1, ultimately leading to macular oedema and visual decline [2]. Therefore, VEGF remains a central therapeutic target in DR, although VEGF also has physiological neuroprotective functions that warrant caution when designing long-term inhibition strategies. Current management of diabetic macular oedema and proliferative DR frequently relies on intravitreal anti-VEGF agents, including bevacizumab, ranibizumab, aflibercept, and, more recently, faricimab. These agents are clinically effective but require invasive, repeated administration and carry procedural risk [3], motivating interest in non-invasive delivery strategies capable of reaching the posterior segment.

The use of natural bioactive compounds is an increasingly attractive approach. Quercetin is the major flavonoid constituent of radish (*Raphanus sativus* L.) leaves, and LC-MS/MS-based profiling has confirmed a high phenolic and flavonoid content, as well as antidiabetic, anti-inflammatory, and anti-haemolytic activities in vitro and in silico [4]. Pharmacologically, quercetin has been reported to inhibit VEGF/VEGFR-mediated angiogenesis in retinal microvascular endothelial cells, reduce VEGF expression in streptozotocin (STZ)-induced diabetic retinas, and protect the retina by inducing haem oxygenase-1, which in turn suppresses VEGF and soluble ICAM-1 [5]. More recently, quercetin was shown to attenuate high-glucose-induced VEGFA expression in ARPE-19 cells by suppressing reactive oxygen species (ROS) generation and p38 MAPK/NF-κB signalling [6]. Earlier work by Sharifi et al. established HPLC-based extraction and quantification of quercetin from R. sativus leaves, providing methodological precedent for the present study [7].

Conventional topical eye drops have very low ocular bioavailability, with reviews commonly reporting that less than 5% of the topically applied dose reaches the intraocular tissue because of blinking, tear turnover, nasolacrimal drainage, and corneal/conjunctival clearance [8,9]. This limitation is particularly relevant for posterior-segment diseases such as DR. Mucoadhesive chitosan nanoparticles can prolong precorneal residence and improve anterior-segment permeation, but they generally do not efficiently penetrate the cornea-conjunctiva barrier to reach the posterior fundus [10],

leaving an important delivery gap. Chitosan nanoparticle systems have nonetheless demonstrated feasibility for ocular drug delivery in other contexts, including meloxicam delivery in a rabbit eye model [11] and macromolecular ophthalmic delivery platforms [12].

Fluorocarbon-modified chitosan (FCS) combines the mucoadhesive and biocompatible properties of chitosan with hydrophobic fluorocarbon domains that promote self-assembly and improve the handling of hydrophobic bioactive compounds. Fluorinated chitosan systems have previously been used to enable transdermal immunotherapy for melanoma [13] and have been reviewed as a promising nanoplatform for cancer drug delivery [14], suggesting that similar amphiphilic behavior could be exploited to enhance ocular-surface retention and controlled release of quercetin.

This study integrated four elements that have generally been examined separately in the literature: (1) an in silico molecular docking screen of quercetin and related flavonols against the VEGF-A crystal structure (PDB 3QTK), benchmarked against the clinically used anti-VEGF agent faricimab and filtered using an ophthalmic drug-likeness rule of thumb [15]; (2) HPLC-quantified quercetin from a local plant source (R. sativus leaves); (3) an FCS nanocarrier characterised physicochemically (particle size, encapsulation efficiency, refractive index, viscosity, ex vivo ocular retention); and (4) an in vivo STZ-induced diabetic rat model evaluating fasting blood glucose and retinal histopathology. The aim was to develop and evaluate a quercetin-FCS eyedrop with emphasis on retinal protection, while explicitly distinguishing computationally predicted VEGF-A affinity from directly measured in vivo VEGF expression, which was not assayed in the present dataset.

This study offers three novel contributions. It provides the first parallel DPPH–ABTS characterisation of S. taccada, advances an explicit hydrophilic–lipophilic interpretation of assay divergence linked to metabolite class, and deliberately frames these data as a formulation-relevant baseline rather than a terminal screening result. The objectives of this study were to qualitatively screen the secondary metabolite profile of S. taccada extract, to determine and compare its radical-scavenging capacity by DPPH and ABTS assays, to analyse the correlation and systematic discrepancy between both assays, and to establish a bioactive baseline that guides subsequent nanostructured lipid carrier development for ocular anticataract application.

2 Material and Methods

2.1 Material

The materials used included fresh Raphanus sativus L. leaves, quercetin reference standard, chitosan, trifluoroacetic acid (TFA), 1-ethyl-3-(3-dimethylaminopropyl) carbodiimide (EDC), N-hydroxysuccinimide (NHS), dimethyl sulfoxide (DMSO), glacial acetic acid, hydrochloric acid, 70% ethanol, phosphate-buffered saline (PBS), water for injection, streptozotocin (STZ), sodium citrate buffer, and male Sprague–Dawley rats. Standard laboratory glassware, an analytical balance, an oven, a blender, and a magnetic stirrer were used.

2.2 In Silico Molecular Docking

The three-dimensional structures of quercetin and the comparator flavonols (myricetin, kaempferol, and apigenin) were retrieved from UniProt/PubChem, and the crystal structure of VEGF-A (PDB ID: 3QTK; Homo sapiens, X-ray diffraction, 1.85 Å resolution, no reported mutation) was retrieved from the RCSB Protein Data Bank. Faricimab, a clinically approved anti-VEGF agent, was used as the reference ligand. Structure files were converted and prepared using AutoDock Tools. Docking was performed in three stages—ligand/protein preparation, construction of an imaginary docking box around the binding site, and docking simulation—using AutoDock Tools, followed by visualisation of the docking poses in LigPlot+ and PyMOL. Binding energy (ΔG) and the predicted inhibition constant (Ki) were used to rank ligand affinity, with more negative ΔG and lower Ki indicating stronger predicted binding. Drug-likeness and pharmacokinetic/toxicity profiles were additionally screened using an ADMETox prediction workflow and evaluated against an ophthalmic drug rule-of-thumb physicochemical space [15]. Protein–ligand interactions (hydrogen bonds, hydrophobic contacts, and van der Waals contacts) were analysed to identify shared binding-pocket residues between quercetin and faricimab.

2.3 Determination and Extraction of R. sativus Leaves Antioxidant Activity Using the DPPH Method

Plant material was authenticated at the Herbarium Medanense plant systematics laboratory. Leaves were washed under running water, oven-dried at 50°C for 7 h, and milled into fine powder. A 150 g portion of the powder was macerated with 1.5 L of 70% ethanol (1:10, w/v) for 72 h at room temperature. The macerate was filtered, and the filtrate was concentrated using a rotary evaporator at 45°C, followed by a water bath at 50°C to obtain a viscous extract, which was stored at 4°C. Organoleptic characteristics, moisture content, and extraction yield were recorded. Phytochemical screening for flavonoids, alkaloids (Wagner and Dragendorff reagents), saponins, tannins, triterpenoids, and phenolics was performed using standard colour/precipitation reactions. Quercetin content in the extract was quantified by high-performance liquid chromatography (HPLC) against a quercetin reference standard using retention time matching for peak identification.

2.4 Synthesis of Fluorocarbon-Modified Chitosan (FCS)

TFA (31.3 mg; 274.7 μmol) was dissolved in 2–3 mL DMSO and activated with EDC/NHS at a 1:2:1 molar ratio. Separately, 200 mg chitosan was dissolved in 20 mL of 1% acetic acid. The activated TFA solution was added dropwise to the chitosan solution, and the mixture was stirred for 12 h in the dark. Hydrochloric acid (1 M, 5 mL) was then added and the mixture was stirred for 30 min. The resulting FCS-HCl precipitate was recovered using cold anhydrous ethanol, washed three times, and freeze-dried to obtain FCS powder. The chemical identity of FCS was verified by Fourier-transform infrared (FTIR) spectroscopy against a chitosan reference spectrum.

2.5 Formulation of Quercetin-FCS Eyedrop

Three formulation variants were prepared using 100 mg (V1/P1), 50 mg (V2/P2), and 25 mg (V3/P3) of R. sativus leaf extract, each dissolved in 6 mL water for injection. FCS was separately dissolved in PBS at 10 mg/mL. The leaf extract and FCS solutions were combined at a 1:1 ratio and homogenised for 10 min using a magnetic stirrer until a uniform mixture was obtained. The pH of each formulation was adjusted toward physiological ocular pH. The formulation composition is summarised in Table 1.

Table 1. Composition of the three quercetin-FCS eyedrop variants.

Component	Function	V1 / P1	V2 / P2	V3 / P3
R. sativus leaf extract	Active ingredient	100 mg	50 mg	25 mg
Fluorocarbon-modified chitosan (FCS)	Drug carrier	10 mg/mL	10 mg/mL	10 mg/mL
Water for injection	Vehicle/solvent	6 mL	6 mL	6 mL

2.6 Physicochemical Characterisation

Each formulation was evaluated for organoleptic appearance (colour, odour, physical form), pH, sterility, viscosity, particle size, encapsulation efficiency (EE%), and refractive index (RI). Sterility was assessed by inoculation onto nutrient agar and inspection for bacterial growth after 24 h of incubation. Particle size was measured using a particle size analyzer (PSA). Encapsulation efficiency was calculated as the proportion of leaf extract successfully entrapped within FCS. Refractive index was measured to evaluate compatibility with ocular administration, with an accepted upper threshold of 1.476 for ocular preparations [16].

2.7 Ex Vivo Ocular Retention Assay

Ocular surface retention was assessed qualitatively using an isolated cornea assay. An excised cornea was placed in a Petri dish and immersed in each formulation pre-mixed with methylene blue dye for 4 h at 37°C. Dye penetration and residual staining intensity were assessed visually as a qualitative indicator of how long each formulation could be expected to persist on the ocular surface before being cleared by nasolacrimal drainage, tear turnover, and blinking [17].

2.8 In Vivo Experimental Design

Fifteen male Sprague–Dawley rats (±8 weeks old, 180–220 g) were acclimatised for 7 days under standard laboratory conditions (25 ± 2°C, 12 h light/dark cycle) with free access to food and water, following a protocol approved by the Health Research Ethics

Committee, Faculty of Medicine and Health Sciences, Universitas Muhammadiyah Sumatera Utara (approval No. 157/KEPK/FKIKUMSU/2026). Animals were randomly allocated into five groups (n = 3 per group): a negative control without STZ induction; a positive diabetic control receiving STZ without treatment; and three treatment groups (P1, P2, P3) receiving STZ followed by eyedrop variants V1, V2, and V3, respectively. Diabetes was induced by intraperitoneal injection of STZ (50 mg/kg body weight) dissolved in 10 mM sodium citrate buffer (pH 4.5) for five consecutive days after overnight fasting; animals with fasting blood glucose ≥ 250 mg/dL were confirmed as diabetic [18]. Treatment groups received the corresponding eyedrop formulation, applied topically to the bulbar conjunctiva at a concentration of 4 mg/mL (0.4% w/v), one drop per eye, twice daily, for 30 days.

2.9 Histopathological Evaluation

At the end of the treatment period, animals were euthanised and both eyes were enucleated, fixed in paraformaldehyde, processed in paraffin, sectioned, and stained with hematoxylin and eosin. Retinal sections were assessed by a blinded observer for five parameters associated with diabetic retinopathy: basal membrane thickening, capillary degeneration, neovascularisation, pericyte degeneration, and microaneurysm formation, each scored per field of view and summed to give a total damage score per eye, following a previously described scoring framework for diabetic retinopathy in rodent models [19].

2.10 Statistical Analysis

Shapiro–Wilk and Levene's tests indicated that the retinal histopathology data were not normally distributed and did not meet the assumption of homogeneity of variance ($p < 0.05$ for both). The Kruskal–Wallis test showed statistically significant differences among the five groups for all histopathological parameters ($p < 0.05$). Post-hoc Mann–Whitney U tests with Bonferroni correction confirmed that P1 had significantly lower retinal damage scores than the positive control and the other treatment groups, supporting a dose-dependent protective effect of the quercetin-FCS eyedrop.

3 Results

The VEGF-A crystal structure (PDB 3QTK) met the quality criteria required for a docking target. Among the four candidate flavonols, quercetin showed the most favourable predicted binding energy and the lowest inhibition constant, second only to the anti-VEGF comparator faricimab (Table 2). ADMETox screening identified quercetin as the only tested compound that satisfied the physicochemical druglikeness criteria of the ophthalmic-drug rule of thumb [15], and interaction analysis showed that quercetin shared several key binding-pocket residues with faricimab (including ARG A:437, LYS A:439, TYR A:617, and VAL A:435), suggesting a biologically plausible, though computationally predicted, basis for a VEGF-A-related mechanism.

Table 2. Molecular docking results of candidate ligands against VEGF-A (PDB 3QTK).

Compound	Binding energy (kcal/mol)	RMSD (Å)	Inhibition constant, Ki (μM)
Quercetin	−8.21	66.07	9.089
Myricetin	−5.49	66.98	12.177
Kaempferol	−4.59	71.68	15.581
Apigenin	−6.67	70.04	29.043
Faricimab (comparator)	−8.93	67.68	7.305

3.1 Extraction and Phytochemical Screening

Maceration of 150 g of dried leaf powder yielded 139.21 g of concentrated extract, corresponding to a 23.20% extraction yield, with a moisture content of 7.85% (within the <10% requirement for herbal simplicia). The extract was dark greenish-black, characteristically odorous, and viscous, consistent with normal maceration output. Phytochemical screening was positive for flavonoids, alkaloids (Wagner and Dragendorff reagents), saponins, tannins, triterpenoids, and phenolics, indicating a phytochemically rich extract consistent with antioxidant and anti-inflammatory potential.

3.2 HPLC Quantification of Quercetin

HPLC analysis confirmed the presence of quercetin in the leaf extract at a concentration of 125.430 ppm, with a retention time of 12.543 min matching the quercetin reference standard, indicating the accurate and specific identification of the target compound in the extract.

3.3 FCS Synthesis and FTIR Characterisation

The synthesis yielded a dry FCS powder following precipitation, washing, and freeze-drying. The FTIR spectrum of FCS closely resembled that of the chitosan standard, with a spectral correlation of 99.48%. Absorption bands at 3000–3500 cm^{-1} corresponded to O–H and N–H stretching, bands at 1500–1600 cm^{-1} corresponded to nitrogen-containing functional groups, and the 1000–1300 cm^{-1} region matched the characteristic chitosan fingerprint region, confirming that FCS retained the core structural features of chitosan after fluorocarbon modification.

3.4 Physicochemical Properties of the Eyedrop Formulations

All three formulations were clear to slightly yellowish, odorless liquids at pH 7 and showed no bacterial growth on nutrient agar after 24 h of incubation. Viscosity decreased with decreasing extract dose (V1 > V2 > V3), remaining within the 2–3 cP range considered appropriate for ocular preparations. Particle size analysis showed a mean particle diameter of 24.67 nm (mean/median ratio 0.949), with the dominant particle population falling within the 1–100 nm nanoscale range. Encapsulation efficiency was highest in V1 (93.85%), followed by V2 (89.57%) and V3 (84.72%), all exceeding the 80% benchmark considered indicative of an efficient nanoencapsulation system [20]. The refractive indices for V1–V3 were all below the 1.476 ocular-compatibility threshold [16]. These results are summarised in Table 3.

Table 3. Physicochemical characteristics of quercetin-FCS eyedrop formulations

Parameter	V1 / P1 (100 mg)	V2 / P2 (50 mg)	V3 / P3 (25 mg)
Appearance	Clear, yellowish	Clear, yellowish	Clear, yellowish
Odour	Odourless	Odourless	Odourless
Physical form	Liquid	Liquid	Liquid
pH	7	7	7
Sterility (24 h, NA)	No growth	No growth	No growth
Viscosity (cP)	2.809	2.505	2.214
Mean particle size (nm)	24.67 (pooled)	–	–
Encapsulation efficiency, EE (%)	93.85	89.57	84.72
Refractive index	1.334448	1.333845	1.333977

3.5 Ex Vivo Ocular Retention

Qualitative ocular retention testing showed the greatest residual methylene-blue staining and, therefore, the longest apparent corneal retention for V1, followed by V2 and V3. This ranking was concordant with the viscosity results, in which V1 also showed the highest viscosity, supporting the interpretation that higher extract/FCS concentration was associated with prolonged ocular surface contact time.

3.6 Fasting Blood Glucose

Before STZ induction, fasting blood glucose (FBG) levels were within the normal range in all groups (mean 110–139 mg/dL). Following five days of STZ induction, FBG levels rose markedly in the positive control and all treatment groups (mean 270–317 mg/dL), confirming successful induction of hyperglycaemia (≥250 mg/dL). After 30 days of topical treatment, FBG declined in all treatment groups, with the largest reduction observed in P1, which received the highest extract dose (Table 4).

Table 4. Fasting blood glucose (FBG) before induction, after STZ induction, and after 30 days of eyedrop therapy.

Group	Pre-STZ (mg/dL)	Post-STZ, 72 h (mg/dL)	Post-therapy, day 30 (mg/dL)	FBG reduction (%)
Negative control	118.33 ± 6.43	–	–	–
Positive diabetic control	139.33 ± 17.24	304.67 ± 27.43	–	–
P1 (100 mg)	110.33 ± 7.51	316.67 ± 24.79	118.67 ± 8.50	62.47 ± 0.45
P2 (50 mg)	118.00 ± 16.09	284.33 ± 11.37	153.33 ± 9.29	46.03 ± 1.82
P3 (25 mg)	112.67 ± 15.50	269.67 ± 19.86	166.67 ± 11.37	38.10 ± 1.80

3.7 Retinal Histopathology

The negative control group showed no retinal injury in either eye (total score 0.00 ± 0.00). The positive diabetic control showed the greatest damage (mean total score 14.33 ± 1.21), driven predominantly by capillary degeneration, neovascularisation, and microaneurysm formation. Among the treatment groups, P1 showed the lowest damage score (4.00 ± 0.63), followed by P2 (9.17 ± 1.17) and P3 (13.67 ± 1.21), indicating a dose-dependent protective trend that mirrored the FBG results (Table 5). Representative haematoxylin–eosin images (Fig. 1) show comparatively preserved retinal architecture in P1 relative to the marked structural abnormalities seen in the positive control.

Table 5. Retinal histopathological damage scores (mean total score per eye, n = 6 eyes/group)

Group	Mean score	SD	Interpretation
Negative control	0.00	0.00	No scored retinal injury
Positive diabetic control	14.33	1.21	Severe injury
P1 (100 mg)	4.00	0.63	Lowest treatment-related injury
P2 (50 mg)	9.17	1.17	Intermediate injury

Group	Mean score	SD	Interpretation
P3 (25 mg)	13.67	1.21	Near diabetic-control injury

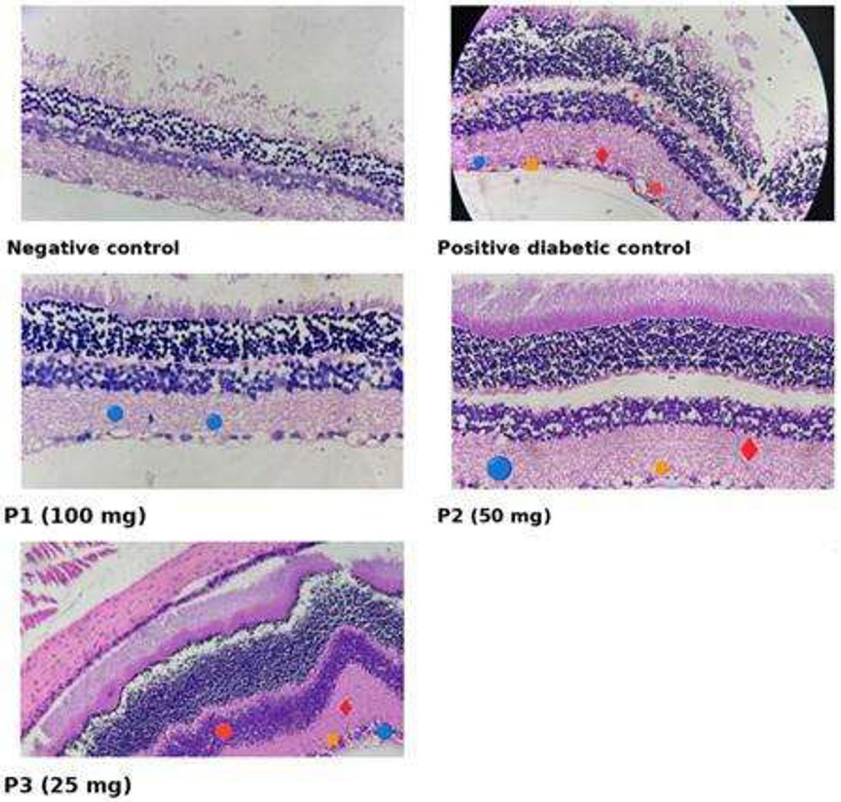


Fig. 1. Representative haematoxylin–eosin-stained retinal sections showing the negative control, positive diabetic control, and P1 (100 mg), P2 (50 mg), and P3 (25 mg) treatment groups

4 Discussion

This revision addresses several methodological gaps identified during the peer review of the earlier draft. First, the quercetin content in the R. sativus leaf extract has now been quantitatively confirmed by HPLC (125.430 ppm; retention time 12.543 min matching the reference standard), rather than inferred solely from a positive phytochemical colour reaction. It is important to note, however, that the 100, 50, and 25 mg doses used to prepare V1–V3 refer to the mass of crude leaf extract incorporated into each formulation, not to isolated quercetin; the HPLC result defines the quercetin concentration within that extract rather than the absolute quercetin dose delivered. Future

work should therefore report an explicit quercetin-equivalent dose (mg quercetin/mg extract × extract mass) alongside the extract-based dosing used here.

Second, the dose description requested by the reviewers has been clarified. The three formulations were prepared from 100, 50, and 25 mg of leaf extract in 6 mL of vehicle, combined 1:1 with 10 mg/mL FCS solution; the resulting eyedrop was applied topically at a concentration of 4 mg/mL (0.4% w/v), one drop per eye, twice daily, for 30 days. A precise per-drop volume and a body-weight-normalised dose (mg/kg/day) were not recorded in the available dataset and are flagged here as a remaining gap rather than estimated retrospectively.

Third, the statistical approach has been revised in response to the concern that one-way ANOVA may not be appropriate for semiquantitative histopathological scores derived from a small sample. Formal testing showed that the retinal damage scores were neither normally distributed nor variance-homogeneous, and the analysis was therefore switched to the non-parametric Kruskal–Wallis test with Mann–Whitney U post-hoc comparisons and Bonferroni correction, which is more appropriate for this type of ordinal, small-sample histopathological data.

Fourth, the mechanistic interpretation has been made more cautious and is now explicitly supported, rather than replaced, by an in silico layer of evidence. Molecular docking indicated that quercetin binds VEGF-A with a predicted affinity second only to faricimab among the tested ligands, sharing several binding-pocket residues with this clinically used anti-VEGF agent, and ADMETox screening identified quercetin as the only candidate meeting an ophthalmic drug-likeness rule of thumb. This computational evidence is consistent with prior reports that quercetin can suppress VEGF/VEGFR-driven angiogenic signalling in retinal endothelial cells, reduce retinal VEGF expression in STZ-induced diabetic rats via haem oxygenase-1 induction, and attenuate high-glucose-induced VEGFA expression in ARPE-19 cells through ROS and p38 MAPK/NF-κB suppression. Nonetheless, docking predictions and literature precedent are not equivalent to a directly measured endpoint: VEGF-A protein or transcript levels were not quantified in the present retinas, and the observed retinal protection may equally reflect quercetin's antioxidant, anti-inflammatory, and antihyperglycaemic activity, individually or in combination. The improved fasting glucose control seen in P1 in particular means that glycaemic and retinal-protective effects cannot be fully disentangled with the present design.

The FCS carrier performed as intended from a formulation perspective. FTIR confirmed retention of the chitosan backbone after fluorocarbon modification, and the resulting nanoformulation had a mean particle size of 24.67 nm, encapsulation efficiency above 84% in every variant, an ocular-compatible refractive index, and a viscosity within the 2–3 cP range considered suitable for ocular surface contact. The ex vivo ocular retention assay and viscosity data were concordant, both ranking V1 as having the longest predicted ocular surface residence time, consistent with the rationale that higher polymer/extract concentration improves mucoadhesive contact time.

The histopathological findings provide the strongest in vivo evidence available. The diabetic positive control showed an approximately 3.6-fold higher damage score than P1, and P1 also produced the largest reduction in fasting blood glucose, with a clear

dose-response relationship across P1–P3 for both endpoints. Compared with intravitreal anti-VEGF therapy, a validated topical formulation would offer an important practical advantage in terms of invasiveness and repeat-dosing burden; however, it would be premature to claim equivalence to established anti-VEGF agents, whose efficacy for diabetic macular oedema is well documented [3]. The principal translational challenge remains achieving adequate posterior-segment exposure while preserving ocular tolerability, an area where mucoadhesive, nanostructured carriers such as FCS are a promising but still unproven approach for this specific application.

The main limitations of this study are the small number of animals per group ($n = 3$, yielding six scored eyes per group) without a documented a priori sample size calculation; the absence of a directly measured in vivo VEGF-A endpoint (ELISA, immunohistochemistry, or qPCR); dosing expressed as extract mass rather than as a quercetin-equivalent or body-weight-normalized dose; and the absence of formal osmolarity, Draize/HET-CAM irritation, pharmacokinetic, and long-term ocular toxicity data. These gaps should be addressed in a confirmatory, adequately powered study before the formulation is proposed for clinical use.

5 Conclusion

A quercetin-containing eyedrop prepared from R. sativus L. leaf extract and encapsulated in fluorocarbon-modified chitosan showed favourable physicochemical properties (24.67 nm mean particle size, 84.72–93.85% encapsulation efficiency, pH 7, ocular-compatible viscosity and refractive index) and dose-dependent in vivo protective effects in an STZ-induced diabetic rat model, with the highest-dose formulation (P1) producing the greatest fasting glucose reduction ($62.47 \pm 0.45\%$) and the lowest retinal histopathological damage score (4.00 ± 0.63) compared with the diabetic control (14.33 ± 1.21; Kruskal–Wallis $p < 0.05$).

In silico molecular docking additionally showed that quercetin has a favourable predicted binding affinity for VEGF-A, second only to the anti-VEGF comparator faricimab among the tested ligands, providing a biologically plausible basis for a VEGF-A-related mechanism. However, because VEGF-A was not directly quantified in the retinal tissue in this study, these findings should be regarded as preliminary evidence of a retinal protective effect rather than definitive proof of VEGF-targeted therapeutic action. Further development should prioritise quantitative VEGF-A assays (ELISA, immunohistochemistry, or qPCR), quercetin-equivalent and body-weight-normalised dosing, an adequately powered confirmatory study, complete nanoparticle characterisation, and ocular safety and pharmacokinetic testing before clinical translation is considered.

Acknowledgments. The authors thank the Directorate of Learning and Student Affairs, Ministry of Higher Education, Science, and Technology of the Republic of Indonesia, for research funding, and the Faculty of Medicine and Health Sciences, Universitas Muhammadiyah Sumatera Utara, for laboratory facilities, academic support, and research ethics facilitation (approval No.

157/KEPK/FKIKUMSU/2026). The authors also thank all contributors involved in the experimental and manuscript-development process.

Disclosure of Interests. The author declared no conflict of interest.

References

1. Genitsaridi, I., Salpea, P., Salim, A., et al.: 11th edition of the IDF Diabetes Atlas: global, regional, and national diabetes prevalence estimates for 2024 and projections for 2050. The Lancet Diabetes and Endocrinology 14(2), 149–156 (2026).
2. Zhang, M., Zhou, M., Cai, X., et al.: VEGF promotes diabetic retinopathy by upregulating the PKC/ET/NF-κB/ICAM-1 signaling pathway. European Journal of Histochemistry 66(4) (2022).
3. Cheema, A.A., et al.: Diabetic macular edema management: a review of anti-vascular endothelial growth factor (VEGF) therapies (2024).
4. Şahin, R.H., Yalçın, E., Çavuşoğlu, K., Özkan, B.: Unveiling the antidiabetic, anti-inflammatory and anti-hemolytic activities of Raphanus sativus leaves through in-vitro and in-silico studies. Scientific Reports 16(1), 1–15 (2026).
5. Chai, G.R., Liu, S., Yang, H.W., Chen, X.L.: Quercetin protects against diabetic retinopathy in rats by inducing heme oxygenase-1 expression. Neural Regeneration Research 16(7), 1344–1350 (2021).
6. Liu, P.K., Chi, Y., Chang, Y., et al.: Quercetin attenuates high glucose-induced VEGFA expression in ARPE-19 cells by inhibiting ROS generation, p38 MAPK phosphorylation, and NF-κB activation. Scientific Reports (2026).
7. Sharifi, N., Mahernia, S., Amanlou, M.: Comparison of different methods in quercetin extraction from leaves of Raphanus sativus L. Pharmaceutical Sciences 23(1), 59–65 (2017).
8. Kompella, U.B., Kadam, R.S., Lee, V.H.L.: Recent advances in ophthalmic drug delivery. Therapeutic Delivery 1(3), 435–456 (2010).
9. Del Amo, E.M., Urtti, A.: Current and future ophthalmic drug delivery systems. Advanced Drug Delivery Reviews 58, 1–24 (2006).
10. Silva, M.M., Calado, R., Marto, J., Bettencourt, A., Almeida, A.J., Gonçalves, L.M.D.: Chitosan nanoparticles as a mucoadhesive drug delivery system for ocular administration. Marine Drugs 15(12), 1–16 (2017).
11. Mohamed, H.B., Shafie, M.A.A., Mekkawy, A.I.: Chitosan nanoparticles for meloxicam ocular delivery: development, in vitro characterization, and in vivo evaluation in a rabbit eye model. Pharmaceutics 14(5) (2022).
12. Shen, J., Gao, H., Chen, L., et al.: Eyedrop-based macromolecular ophthalmic drug delivery for ocular fundus disease treatment. Science Advances 9(4), 1–19 (2023).
13. Fluorocarbon modified chitosan to enable transdermal immunotherapy for melanoma treatment. Small (2023). doi:10.1002/smll.202303634.
14. [14] Kapoor, U.D., Pareek, A., Patel, S., et al.: Advances in cancer therapy using fluorinated chitosan: a promising nanoplatform for drug delivery. Medical Oncology 42, 452 (2025).
15. Karami, T.K., Hailu, S., Feng, S., Graham, R., Gukasyan, H.J.: Eyes on Lipinski's Rule of Five: a new 'rule of thumb' for physicochemical design space of ophthalmic drugs. Journal of Ocular Pharmacology and Therapeutics 38(1), 43–55 (2022).
16. Ahmed, S., Amin, M.M., Sayed, S.: Ocular drug delivery: a comprehensive review. AAPS PharmSciTech 24(2) (2023).

17. Chan, W., Akhbanbetova, A., Quantock, A.J., Heard, C.M.: Topical delivery of a Rho-kinase inhibitor to the cornea via mucoadhesive film. European Journal of Pharmaceutical Sciences 91, 256–264 (2016).
18. Ghasemi, A., Jeddi, S.: Streptozotocin as a tool for induction of rat models of diabetes: a practical guide. EXCLI Journal 22, 274–294 (2023).
19. Canz, M.J., Bagunà-Torres, J., Huerta, J., et al.: Diabetic retinopathy features in Lund MetS rats. Experimental Eye Research 252 (2025).
20. Ganesan, A., Rengarajan, J.: Green synthesis of chitosan nanoparticles using Cassia fistula leaf extract: evaluation of antimicrobial, antioxidant, antibiofilm, and cytotoxic activities. 3 Biotech 14(10), 1–17 (2024).

Open Access This chapter is licensed under the terms of the Creative Commons Attribution-NonCommercial 4.0 International License (http://creativecommons.org/licenses/by-nc/4.0/), which permits any noncommercial use, sharing, adaptation, distribution and reproduction in any medium or format, as long as you give appropriate credit to the original author(s) and the source, provide a link to the Creative Commons license and indicate if changes were made.

The images or other third party material in this chapter are included in the chapter's Creative Commons license, unless indicated otherwise in a credit line to the material. If material is not included in the chapter's Creative Commons license and your intended use is not permitted by statutory regulation or exceeds the permitted use, you will need to obtain permission directly from the copyright holder.

